

Supporting Information

Mechanochromic Optical Sensor Based on Bragg Reflection for Real-time Monitoring of Large-range Sharp Pressure Fluctuations in Aqueous Fluid

Wenxiang Zheng^a, Zhenkun Tan^b, Jing Fan^a, Zihui Meng^a, Mindi Zhang^{b*}, Biao Huang^b, Xiyu Jia^c, Feng Ma^c, Wei Zhu^{c*}, Shushan Wang^c and Lili Qiu^{a*}.

The introduction of cavitation

Cavitation is a hydrodynamic phenomenon that not only affects the behaviors of aquatic organisms, but also has great impact on human activities in hydraulic machinery,^{1,2} ship engineering^{3,4} and underwater explosion⁵. The formation of cavitation bubbles is a phase transition process that water turns into vapor when the local pressure drops below the saturated vapor pressure of water⁶. Therefore, any method that can generate low pressure in liquid has the potential to create cavitation bubbles. The evolution of cavitation bubbles undergoes four stages of expansion, shrinkage, collapse and rebound^{7,8}, the high-velocity jets in the shrinkage and collapse processes and the shock waves with huge energy generated during the rebound process can cause structural vibration⁹, damage¹⁰ and even fracture¹¹, which attracted the attention of researchers in more than a century. High-velocity jets and shock waves are considered to be the main factors causing destructive damage. At present, high-speed cameras are mostly used to study High-velocity jets¹²⁻¹⁴. Furthermore, researchers developed optical methods and devices to research the propagation of shock waves and their pressure^{15,16}. However, these methods cannot observe and measure the loading characteristics of near the boundary of cavitation. Therefore, a convenient and fast method for realize the quantification of cavitation bubble loads is urgently needed to promote the further research and development of cavitation phenomenon.

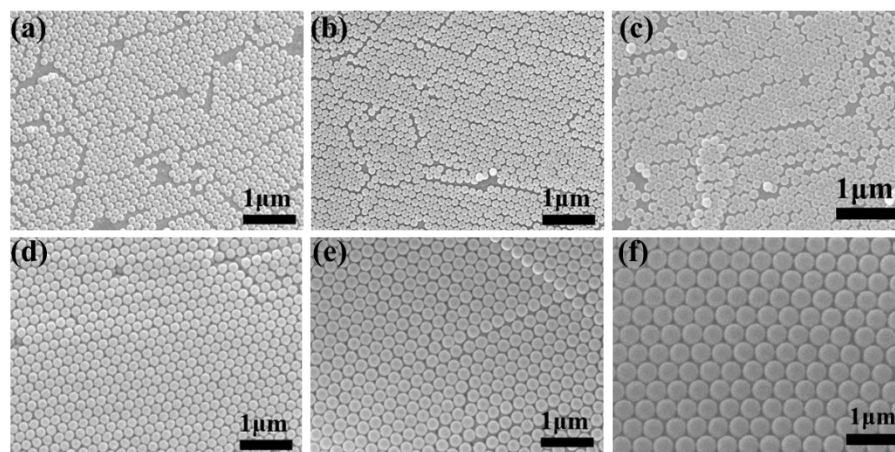


Figure S1. The SEM of PMMA (a)126 nm; (b)137 nm;(c)150 nm; (d)190 nm; (e) 230 nm; (f)255nm.

The BIS, DEAP and AM prepared NPCs hydrogel also influence the zeta potential and electrostatic interaction strength. The amounts of BIS (1.67wt%) and DEAP ($5\mu\text{L}\cdot\text{g}^{-1}$) in the preparation of NPCs barely affected the zeta potential of PMMA microspheres (Fig. S2a and S2b). As shown in Fig. S2c, AM showed prominent effect on the zeta

potential. The zeta potential decreased significantly and was below 43mV at m AM: m PMMA = 100wt%. The BIS (1.67wt%), DEAP ($5\mu\text{L}\cdot\text{g}^{-1}$), AM (58.3wt%) and ion exchange resin were sequentially added into PMMA suspensions (Fig.S2d), the zeta potential decreased slightly with 1.67wt% BIS and changed from -52.5 mV to -46.0 mV with 58.3wt% AM, the $5\mu\text{L}\cdot\text{g}^{-1}$ DEAP had little effect on zeta potential, which was consistent with the results in Fig. S2a-c. The ion exchange resin changed to -51 mV and enhanced the electrostatic interaction between PMMA microspheres, which was conducive to the preparation of high-quality NPCs hydrogel.

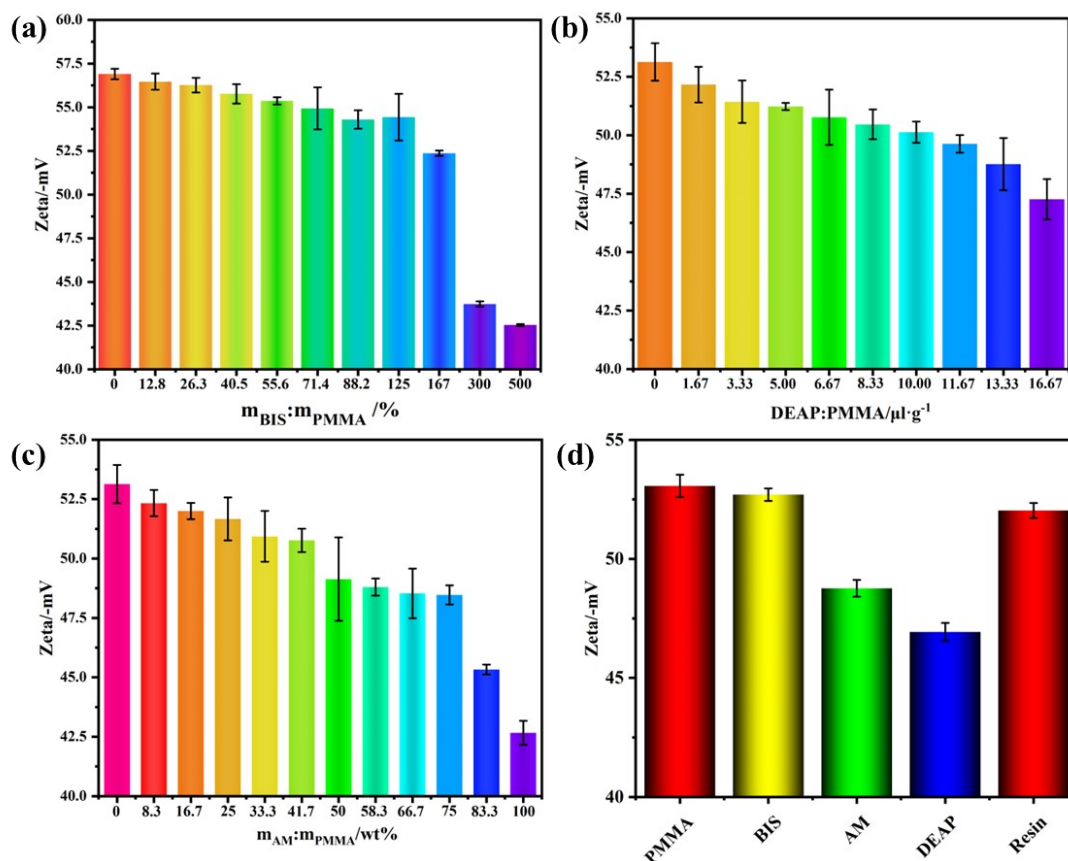


Figure S2. The effects of (a) BIS, (b) DEAP and (c) AM on zeta potential of PMMA microspheres; (d) zeta potential of adding 1.67wt% BIS, 58.3wt % AM, $5\mu\text{L}\cdot\text{g}^{-1}$ DEAP and ion exchange resin to 0.1wt% 126 nm PMMA in turn.

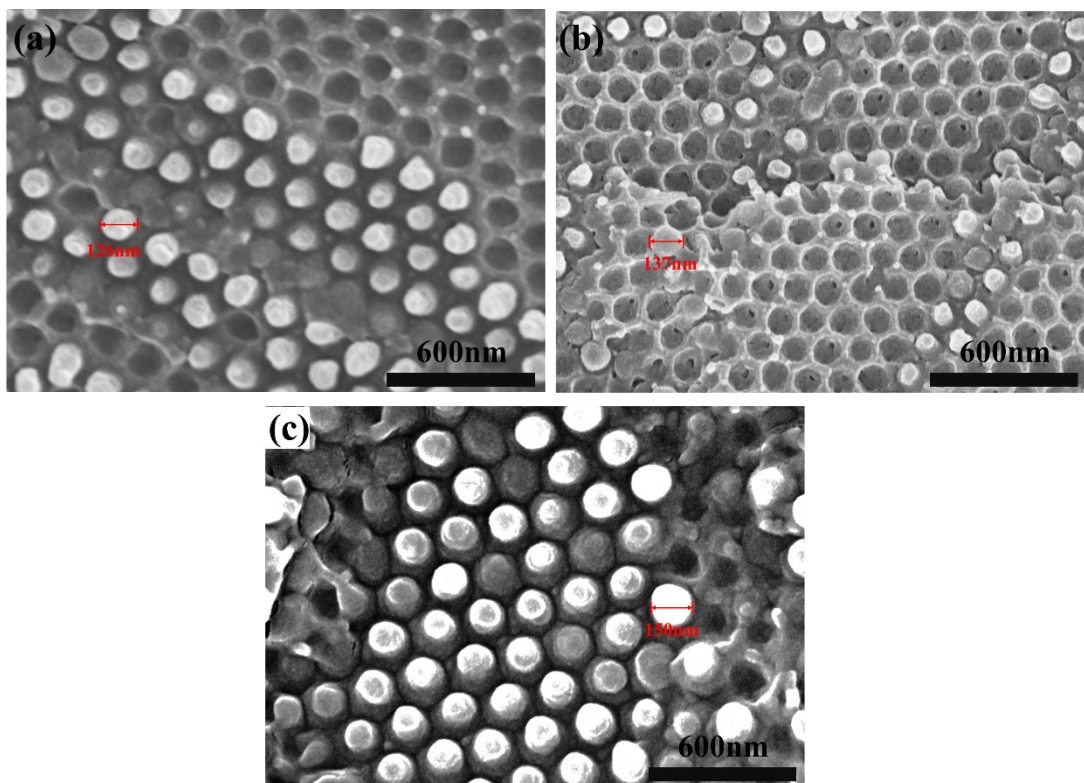


Figure S3. The SEM of the NPCs hydrogels (a) 126 nm, (b)137 nm and (c)150 nm 18wt% PMMA microspheres.

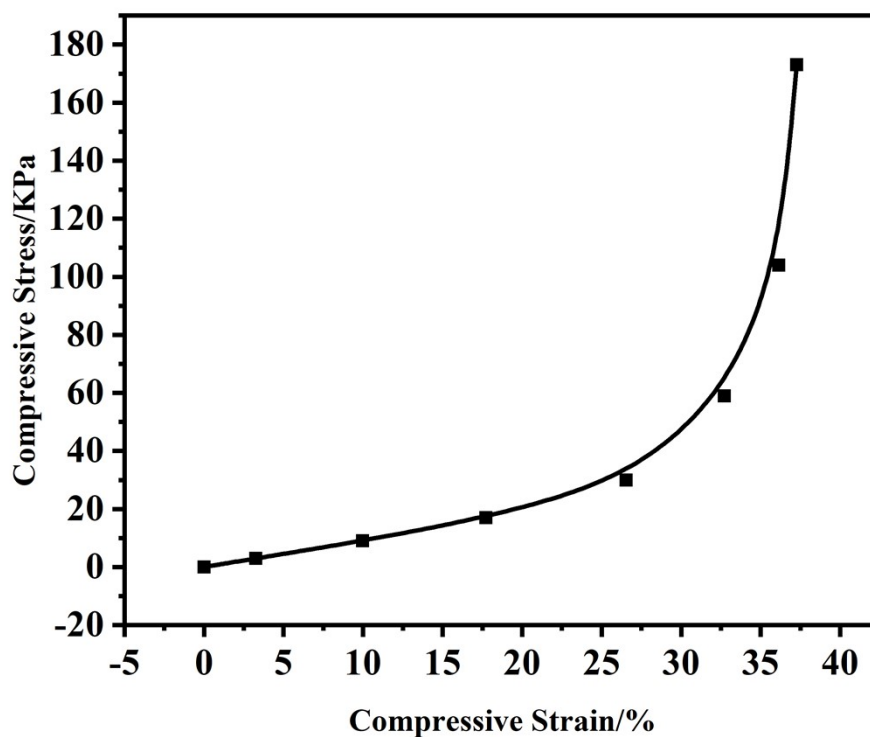


Figure S4. The strain-pressure curve calculated from Equation (1) and the reflection peak in Figure 2j

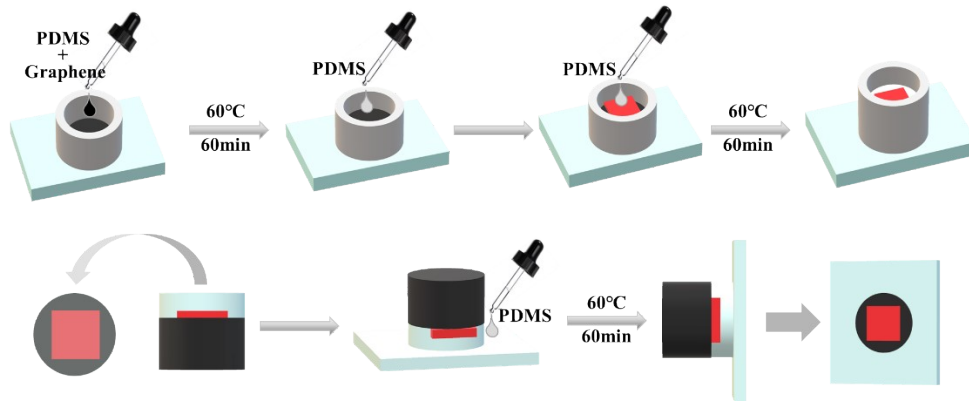


Figure S5. The construction of the mechanochromic optical sensor for the monitoring of large-scale pressure fluctuation in the aqueous fluid.

Table S1. Correspondence between Zeta potential and system stability

Zeta potential/mV	Colloidal system stability
0~±5	Condensation or aggregation rapidly
±10~±30	Start to become unstable
±30~±40	General stability
±40~±60	Good stability
Over ±60	Excellent stability

References

- [1] X.-w. Luo, B. Ji and Y. Tsujimoto, *Journal of Hydrodynamics*, 2016, **28**, 335-358.
- [2] B. Huang, Y. L. Young, G. Wang and W. Shyy, *Journal of Fluids Engineering*, 2013, **135**.
- [3] C. Park, G. D. Kim, G.-T. Yim, Y. Park and I. Moon, *Ocean Engineering*, 2020, **213**, 107655.
- [4] Ç. S. Köksal, O. Usta, B. Aktas, M. Atlar and E. Korkut, *Ocean Engineering*, 2021, **239**, 109820.
- [5] A. M. Zhang, S. Li and J. Cui, *Physics of Fluids*, 2015, **27**, 062102.
- [6] X. Ma, B. Huang, X. Zhao, Y. Wang, Q. Chang, S. Qiu, X. Fu and G. Wang, *Ultrasonics Sonochemistry*, 2018, **43**, 80-90.
- [7] W. Lauterborn and C.-D. Ohl, *Ultrasonics Sonochemistry*, 1997, **4**, 65-75.
- [8] P. B. Robinson, J. R. Blake, T. Kodama, A. Shima and Y. Tomita, *Journal of Applied Physics*, 2001, **89**, 8225-8237.
- [9] G. Huang, M. Zhang, X. Ma, Q. Chang, C. Zheng and B. Huang, *Ultrasonics Sonochemistry*, 2020, **67**, 105147.
- [10] B. Huang, Y. Zhao and G. Wang, *Computers & Fluids*, 2014, **92**, 113-124.
- [11] T. Sun, Z. Wang, L. Zou and H. Wang, *Ocean Engineering*, 2020, **197**, 106831.
- [12] P. Cui, A. M. Zhang, S. Wang and B. C. Khoo, *Journal of Fluid Mechanics*, 2018, **841**, 287-309.
- [13] P. Cui, A. M. Zhang, S.-P. Wang and Y.-L. Liu, *Journal of Fluid Mechanics*, 2020, **897**, A25.
- [14] B. H. T. Goh, S. W. Ohl, E. Klaseboer and B. C. Khoo, *Physics of Fluids*, 2014, **26**, 042103.
- [15] Y. Tomita, T. Kodama and A. Shima, *Applied Physics Letters*, 1991, **59**, 274-276.
- [16] W.-L. Xu, J.-B. Li, J. Luo and Y.-W. Zhai, *Experimental Thermal and Fluid Science*, 2021, **120**, 110218.